About the Author

Dr. LaFleur is an assistant professor at the University of San Diego, California, USA, and the founder and director of Lemur Love, a US-based nonprofit organization conducting research, conservation, and small-scale development in Madagascar. Her research examines the ecology of wild ring-tailed lemurs and the legal and illegal trades of wild-captured lemurs in Madagascar.

References

1. Blancou J, Rakotoniaina P, Cheneau Y. Types of TB bacteria in humans and animals in Madagascar [in French]. Arch Inst Pasteur Madagascar. 1974;43:31–38.
2. Ligthelm LJ, Nicol MP, Hoek KGP, Jacobson R, van Helden PD, Marais BJ, et al. Xpert MTB/RIF for rapid diagnosis of tuberculous lymphadenitis from fine-needle-aspiration biopsy specimens. J Clin Microbiol. 2011; 49:3967–70. https://doi.org/10.1128/JCM.01310-11
3. Hunt M, Bradley P, Lapierre SG, Heys S, Thomsit M, Hall MB, et al. Antibiotic resistance prediction for *Mycobacterium tuberculosis* from genome sequence data with Mykrobe. Wellcome Open Res. 2019;4:191. https://doi.org/10.12688/wellcomeopenres.15603.1
4. Shitikov E, Kolchenko S, Mokrousov I, Bespyatykh J, Ischenko D, Ilina E, et al. Evolutionary pathway analysis and unified classification of East Asian lineage of *Mycobacterium tuberculosis*. Sci Rep. 2017;7:9227. https://doi.org/10.1038/s41598-017-10018-5
5. Rutaihwa LK, Menardo F, Stucki D, Gygli SM, Ley SD, Malla B, et al. Multiple introductions of *Mycobacterium tuberculosis* lineage 2–Beijing into Africa over centuries. Front Ecol Evol. 2019;7:112. https://doi.org/10.3389/fevo.2019.00112
6. Stucki D, Brites D, Jeljeli L, Coscolla M, Liu Q, Trauner A, et al. *Mycobacterium tuberculosis* lineage 4 comprises globally distributed and geographically restricted sublineages. Nat Genet. 2016;48:1535–43. https://doi.org/10.1038/ng.3704
7. Ferdinand S, Sola C, Chanteau S, Ramarokoto H, Rasolonavalona T, Rasolofo-Razanamparany V, et al. A study of spoligotyping-defined *Mycobacterium tuberculosis* clades in relation to the origin of peopling and the demographic history in Madagascar. Infect Genet Evol. 2005;5:340–8. https://doi.org/10.1016/j.meegid.2004.10.002
8. LaFleur M, Clarke TA, Reuter KE, Schaefer MS, terHorst C. Illegal trade of wild-captured *Lemur catta* within Madagascar. Folia Primatol (Basel). 2019;90:199–214. https://doi.org/10.1159/000496970
9. Reuter KE, LaFleur M, Clarke TA, Holiniaina Kjeldgaard F, Ramanantenasoa I, Ratolojanahary T, et al. A national survey of household pet lemur ownership in Madagascar. PLoS One. 2019;14:e0216593. https://doi.org/10.1371/journal.pone.0216593
10. Chomel BB, Belotto A, Meslin FX. Wildlife, exotic pets, and emerging zoonoses. Emerg Infect Dis. 2007;13:6–11. https://doi.org/10.3201/eid1301.060480

Address for correspondence: Marni LaFleur, Department of Anthropology, University of San Diego, Saints Tekawitha-Serra Hall, Suite 218C, 5998 Alcala Park, San Diego, CA 92110-2492, USA; email: marni.lafleur@gmail.com

Genomic and Pathologic Findings for *Prototheca cutis* Infection in Cat

Grazieli Maboni,[1] Jessica A. Elbert,[1] Justin M. Stilwell, Susan Sanchez

Author affiliations: University of Guelph, Guelph, Ontario, Canada (G. Maboni); Athens Veterinary Diagnostic Laboratory, Athens, Georgia, USA (G. Maboni, S. Sanchez); University of Georgia, Athens (J.A. Elbert, J.M. Stilwell)

DOI: https://doi.org/10.3201/eid2703.202941

Severe nasal *Prototheca cutis* infection was diagnosed postmortem for an immunocompetent cat with respiratory signs. Pathologic examination and whole-genome sequencing identified this species of algae, and susceptibility testing determined antimicrobial resistance patterns. *P. cutis* infection should be a differential diagnosis for soft tissue infections of mammals.

Prototheca spp. (phylum Chlorophyta, order Chlorellales, family *Chlorellaceae*) are ubiquitous algal organisms that represent emerging infectious agents of humans and animals (*1*). Protothecosis has been increasingly reported for immunocompromised human and animal patients (*1*,*2*). At least 14 species of *Prototheca* have been recognized; 1 case of *P. cutis*–associated dermatitis in an immunocompromised man has been reported (*3*,*4*). We describe a case of *P. cutis* in a domestic cat in Georgia, USA.

In January 2020, an 11-year-old, 5.8-kg, neutered male, domestic cat was examined for sneezing, wheezing, congestion, and rhinitis. This indoor/outdoor cat was negative for feline leukemia and feline immunodeficiency viruses. The cat showed no response to treatment with steroids and cefovecin sodium (Convenia; Zoetis, https://www.zoetis.com). From June 2019 through January 2020, the nasal planum became rounded and disfigured. A biopsy sample submitted to a private diagnostic laboratory indicated a fungal infection containing organisms suggestive of *Cryptococcus* spp. Because of concerns over the zoonotic potential of *Cryptococcus* spp., the cat was euthanized and submitted for postmortem examination.

Gross reflection of the skin revealed that a locally extensive area of connective tissue and musculature overlying ≈70% of the nasal bridge and dorsal nasal planum was diffusely soft, variably tan to light orange, and mildly gelatinous (Appendix Figure 1, https://wwwnc.cdc.gov/EID/article/27/3/20-2941-App1.pdf).

[1]These authors contributed equally to this article.

Microscopic evaluation revealed a severe granulomatous nodular dermatitis, panniculitis, cellulitis, pyogranulomatous osteomyelitis, and rhinitis (Figure). Disseminated throughout the nasal turbinates were numerous free and intrahistiocytic sporangia with and without endospores (Figure). Although these findings suggest previously resolved infection in the skin, subcutis, and muscle and active infection in the nasal turbinates, the initial site of infection (cutaneous vs. nasal turbinates) and disease pathogenesis could not be definitively determined (Appendix).

Fungal culture yielded white colonies growing in the presence and absence of light at 30°C (Appendix Figure 2). Cytologic examination revealed colonies of round cells with internal septations and thick walls resembling sporangia and endospores, which were identified with lactophenol cotton blue stain (Appendix Figure 2). Sporangia were gram positive, although they appeared to be unevenly stained (Appendix Figure 2). Genus and species were not identified by matrix-assisted laser desorption ionization/time-of-flight mass spectrometry and GEN III Microbial identification (Biolog, https://www.biolog.com). Partial sequencing of the internal transcribed spacer region and the D1/D2 region of the 28S rRNA gene yielded sequences 96% and 99% homologous to those from *P. cutis* available in BLAST (https://blast.ncbi.nlm.nih.gov) and CBS-KNAW (https://www.knaw.nl, currently Westerdijk Fungal Biodiversity Institute) databases.

Because the mitochondrial *cytb* gene potentially represents a new standard method for identifying *Prototheca* species (*5*), we performed whole-genome sequencing to investigate *cytb* as well as other genes by using Illumina MiSeq (https://www.illumina.com) (Appendix). The nuclear genome was 19,237,076-bp long, and the plastid genome was 51,673-bp long, which corresponds to genome sizes obtained from sequencing of *P. cutis* JCM15793 strain ATCC PRA-138 (https://www.atcc.org) (*6*). We

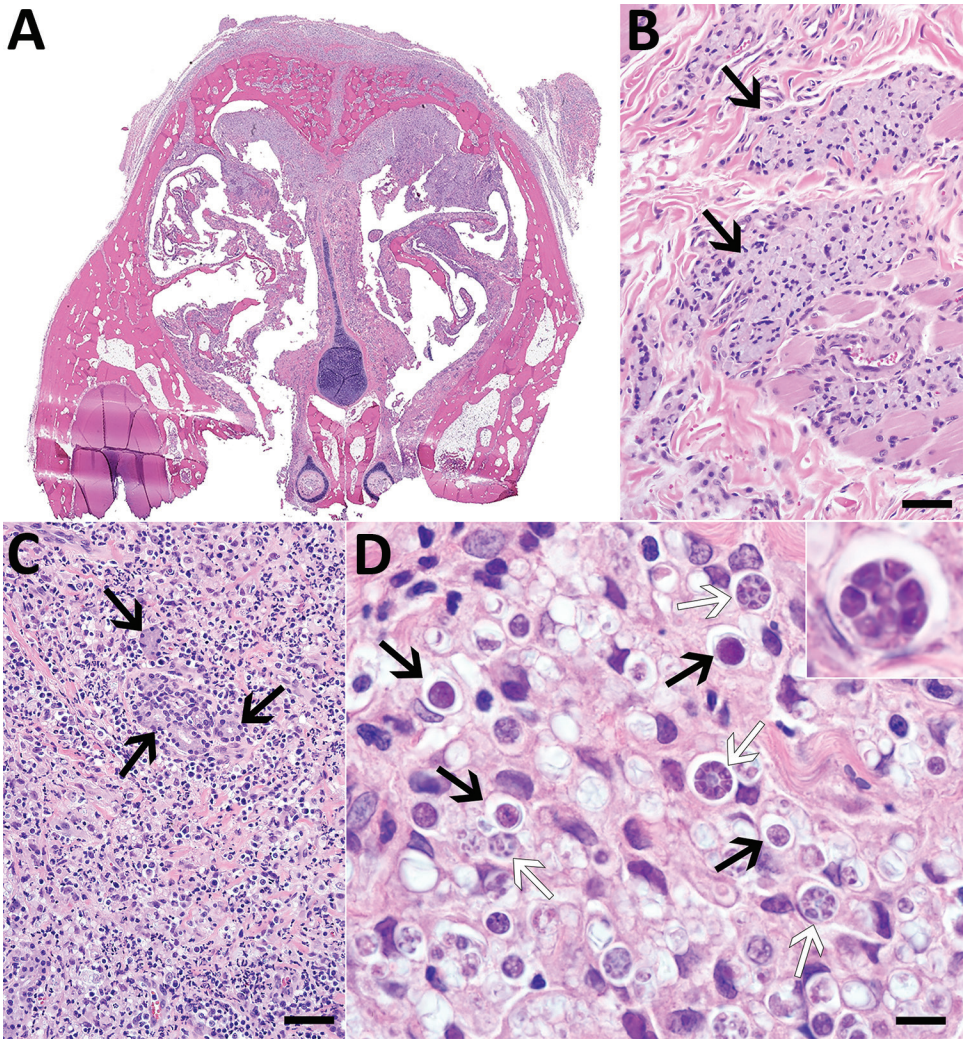

Figure. Histologic lesions associated with protothecosis caused by *Prototheca cutis* in a cat. A) Subgross cross-section of the nasal turbinates showing marked expansion of the nasal epithelium and overlying subcutaneous tissue. B) Epithelioid macrophages (arrows) with abundant, intracytoplasmic, gray material multifocally dissecting through subdermal collagen and musculature. Hematoxylin and eosin (H&E) stain; scale bar indicates 50 µm. C) Submucosal glands (arrows), markedly displaced by myriad macrophages, neutrophils, lymphocytes, plasma cells, and algal sporangia. H&E stain; scale bar indicates 50 µm. D) Algal sporangia (black arrows), which sometimes endosporulate (white arrows), producing up to 8 endospores (inset). H&E stain; scale bar indicates 10 µm and does not apply to inset.

submitted the genome assembly to GenBank (accession no. JABBYS000000000). The in silico–targeted gene alignment revealed genes homologous with available *P. cutis* sequences including *cytB* (99.8%, accession no. MT363977), chloroplast genome DNA (99.54%), 18S rRNA gene (100%, accession no. MT360051), ITS (99.12%, accession no. MT359908), and 28S rRNA (D1/D2 domain) (100%, accession no. MT360265), which were deposited in GenBank.

We performed susceptibility testing for antifungal and antimicrobial drugs because both have been used against *Prototheca* spp. infections in animals (*7*,*8*). The isolate showed high MICs for fluconazole and itraconazole and a low MIC for amphotericin B (Table). Resistance to fluconazole and susceptibility to amphotericin B are well recognized for other *Prototheca* species (*9*); however, resistance to itraconazole could be unique to *P. cutis*. MICs were high for most antimicrobial drugs, including cefovecin, which had been unsuccessful in treating the cat (Table). Oxacillin, pradofloxacin, and trimethoprim/sulfamethoxazole inhibited growth at the lowest concentrations, indicating in vitro sensitivity to these drugs. We further investigated whether resistance genes from the whole-genome sequence corresponded to phenotypic resistance. We used the Comprehensive Antibiotic Resistance Database (https://card.mcmaster.ca) to identify genes conferring resistance to β-lactams, tetracyclines, aminoglycosides, chloramphenicol, and vancomycin. Consistent with MICs, no resistance genes corresponded to pradofloxacin and trimethoprim/sulfamethoxazole (Table). The MIC data provided here may be helpful for establishing future clinical breakpoints for *Prototheca* spp.

Our primary concern with regard to this case was determining the zoonotic potential of the agent, which was initially misdiagnosed as *Cryptococcus* spp. Although *Prototheca* spp. are widely considered to be zoonotic agents, reports of definitive cases of

Table. Antimicrobial and antifungal MICs and resistance genes identified by whole-genome sequencing of *Prototheca cutis* isolated from a nasal lesion in a cat*

Class	MIC, μg/mL	AMR genes
Antimicrobial testing†		
β-lactams		*Oxa-168, NmcA, OXA-198, IMP-8*
Amoxicillin/clavulanate	8	
Ampicillin	>8	
Oxacillin	≤0.25	
Penicillin G	8	
Cefazolin	>4	
Cefovecin	>8	
Cefpodoxime	>8	
Cephalothin	>4	
Imipenem	4	
Tetracyclines		*tet(31)*
Doxycycline	>0.5	
Minocycline	1	
Tetracycline	>1	
Quinolones		None found
Enrofloxacin	>4	
Marbofloxacin	2	
Pradofloxacin	≤0.25	
Aminoglycosides		*AAC(6')-Ij, AAC(3)-Xa, AAC(3)-VIIIa*
Amikacin	>32	
Gentamicin	8	
Lincosamides: clindamycin	4	None found
Macrolides: erythromycin	>4	None found
Rifamycins: rifampin	>2	None found
Nitrofurans: nitrofurantoin	>64	None found
Phenicols: chloramphenicol	>32	*catB10*
Sulfonamides: trimethoprim/sulfamethosoxazole	≤2	None found
Vancomycin	>16	*vanA, vanRO*
Antifungal testing‡		Not investigated
Azoles		
Fluconazol	>256	
Itraconazol	>32	
Polyenes: amphotericin B	0.19	

*AMR genes were identified by using the Comprehensive Antibiotic Resistance Database (https://card.mcmaster.ca). Interpretation of MICs was not included in this table because clinical breakpoints for *Prototheca* spp. are not available. AMR, antimicrobial resistance.
†Antimicrobial susceptibility testing was performed by using a Trek Sensititre Gram Positive panel (TREK Diagnostic Systems, http://www.trekds.com).
‡Antifungal susceptibility testing was performed by using MIC test strips (Liofilchem, https://www.liofilchem.com).

zoonotic transmission are lacking in the literature. Zoonotic transmission from bovids is thought to occur via consumption of contaminated milk (*10*). The zoonotic potential of *P. cutis* is unclear; infectivity is probably similar to that of other *Prototheca* spp.

Our report of *P. cutis* isolation from a cat reinforces protothecosis as an emerging infectious disease of humans and animals. We emphasize the potential of *P. cutis* to infect presumably immunocompetent hosts. The veterinary and human medical communities should be aware of the unusual clinical, pathologic, and microbiological manifestations of protothecosis.

Acknowledgments

We thank the talented histology and microbiology technicians at the Athens Veterinary Diagnostic Laboratory for their technical assistance, especially Paula Bartlett and Amy McKinney.

About the Author

Dr. Maboni is a board-certified veterinary microbiologist working as an assistant professor at the University of Guelph, Canada. Her primary research interests are medical diagnosis of bacterial and fungal diseases.

References

1. Pal M, Abraha A, Rahman MT, Dave P. Protothecosis: an emerging algal disease of humans and animals [cited 2020 Jun 17]. https://www.researchgate.net/publication/266359627_Protothecosis_an_emerging_algal_disease_of_humans_and_animals
2. Lanotte P, Baty G, Senecal D, Dartigeas C, Bailly E, Duong TH, et al. Fatal algaemia in patient with chronic lymphocytic leukemia. Emerg Infect Dis. 2009;15:1129–30. https://doi.org/10.3201/eid1507.090373
3. Jagielski T, Bakula Z, Gawor J, Maciszewski K, Kusber WH, Dylag M, et al. The genus *Prototheca* (Trebouxiophyceae, Chlorophyta) revisited: implications from molecular taxonomic studies. Algal Res. 2019;43:101639. https://doi.org/10.1016/j.algal.2019.101639
4. Satoh K, Ooe K, Nagayama H, Makimura K. *Prototheca cutis* sp. nov., a newly discovered pathogen of protothecosis isolated from inflamed human skin. Int J Syst Evol Microbiol. 2010;60:1236–40. https://doi.org/10.1099/ijs.0.016402-0
5. Jagielski T, Gawor J, Bakuła Z, Decewicz P, Maciszewski K, Karnkowska A. *cytb* as a new genetic marker for differentiation of *Prototheca* species. J Clin Microbiol. 2018;56:e00584–18. https://doi.org/10.1128/JCM.00584-18
6. Suzuki S, Endoh R, Manabe RI, Ohkuma M, Hirakawa Y. Multiple losses of photosynthesis and convergent reductive genome evolution in the colourless green algae *Prototheca*. Sci Rep. 2018;8:940. https://doi.org/10.1038/s41598-017-18378-8
7. Pressler BM, Gookin JL, Sykes JE, Wolf AM, Vaden SL. Urinary tract manifestations of protothecosis in dogs. J Vet Intern Med. 2005;19:115–9. https://doi.org/10.1111/j.1939-1676.2005.tb02669.x
8. Vince AR, Pinard C, Ogilvie AT, Tan EO, Abrams-Ogg AC. Protothecosis in a dog. Can Vet J. 2014;55:950–4.
9. Marques S, Silva E, Carvalheira J, Thompson G. Short communication: in vitro antimicrobial susceptibility of *Prototheca wickerhamii* and *Prototheca zopfii* isolated from bovine mastitis. J Dairy Sci. 2006;89:4202–4. https://doi.org/10.3168/jds.S0022-0302(06)72465-1
10. Melville PA, Watanabe ET, Benites NR, Ribeiro AR, Silva JA, Garino Junior F, et al. Evaluation of the susceptibility of *Prototheca zopfii* to milk pasteurization. Mycopathologia. 1999;146:79–82. https://doi.org/10.1023/A:1007005729711

Address for correspondence: Grazieli Maboni, Department of Pathobiology, Ontario Veterinary College, University of Guelph, 50 Stone Rd E, Guelph, ON N1G 2W1, Canada; email: grazieli.maboni@gmail.com

Validity of Diagnosis Code–Based Claims to Identify Pulmonary NTM Disease in Bronchiectasis Patients

Jennifer H. Ku, Emily M. Henkle, Kathleen F. Carlson, Miguel Marino, Kevin L. Winthrop

Author affiliations: Oregon Health & Science University–Portland State University School of Public Health, Portland, Oregon, USA (J.H. Ku, E.M. Henkle, K.F. Carlson, M. Marino, K.L. Winthrop); Veterans Affairs Portland Healthcare System, Portland (K.F. Carlson)

DOI: https://doi.org/10.3201/eid2703.203124

Nontuberculous mycobacteria infection is increasing in incidence and can lead to chronic, debilitating pulmonary disease. We investigated the accuracy of diagnosis code–based nontuberculous mycobacteria lung disease claims among Medicare beneficiaries in the United States. We observed that these claims have moderate validity, but given their low sensitivity, incidence might be underestimated.

Nontuberculous mycobacteria (NTM) infection is an illness of increasing incidence caused by environmental organisms and can lead to chronic pulmonary disease (*1*–*5*). The accuracy of International

Article DOI: https://doi.org/10.3201/eid2703.202941

Genomic and Pathologic Findings for *Prototheca cutis* Infection in Cat

Appendix

Gross and histopathologic descriptions, fungal culture, phenotypic identification, antimicrobial and antifungal susceptibility testing, Sanger sequencing, and whole genome sequencing.

1. Gross and histopathologic descriptions

Grossly, the dorsal nasal planum and nasal bridge was irregularly rounded, enlarged, and bulging with simple interrupted sutures closing the previous biopsy site. A locally extensive area of connective tissue and musculature overlying ≈70% of the nasal bridge and dorsal nasal planum was diffusely soft, variably tan to light orange, and mildly gelatinous. The subjacent nasal turbinates were mildly swollen, red, and soft. Histologic evaluation of the dermis and subcutis overlying the nasal bridge revealed a multifocal to coalescing, nodular, densely cellular population composed predominantly of epithelioid macrophages filled with intracytoplasmic amorphous, gray material. The inflammatory population extended through the underlying bone and disrupted and effaced the submucosa and mucosa of ≈70% of the dorsal nasal turbinates, resulting in multiple, locally extensive areas of ulcerated mucosa, displacement of submucosal glands, and turbinate bone loss. The macrophages in the nasal turbinates were admixed with few degenerate and non-degenerate neutrophils, lymphocytes, plasma cells, multinucleated giant cells, and rare eosinophils and Mott cells. Scattered throughout the inflammation were numerous, extracellular and intrahistiocytic, round to oval, 8–20 μm diameter algal sporangia that had a clear, 2–4 μm thick wall and contained either a central basophilic nucleus or multiple (2–8) wedge-shaped, radially arranged endospores. Algal cell walls were strongly positive in Periodic acid–Schiff and Grocott-Gomori's methenamine silver stains. Luminal spaces within the nasal cavity contained variable aggregates of the previously described inflammatory population and free algal sporangia admixed with scant hemorrhage and mucin. Variable amounts of necrosis, fibrin, and scant hemorrhage were scattered throughout all affected regions. Other histologic

findings unrelated to algal infection included segmental, lymphoplasmacytic and eosinophilic enteritis, renal cortical cysts with lymphocytic interstitial nephritis, nodular adrenal cortical hyperplasia, and presumptive Sarcocystosis within the skeletal and cardiac muscle.

The definitive pathogenesis of protothecosis is unknown. One possible route of infection is traumatic cutaneous inoculation from a penetrating injury, which is consistent with previous reports of Protothecosis in cats (*1*). Macrophages within the dermis, subcutis, and bone contained intracytoplasmic gray material presumptively representing phagocytosed sporangial walls post endosporulation, which was seen actively occurring within in the nasal turbinates. Given the length of time between initial infection and presentation to necropsy, the findings suggest the inoculating wound and initial site of infection could have been removed via biopsy or resolved with subsequent dissemination of the pathogen deeper into the subcutis and nasal turbinates. Another possibility reflects infection via the nasal cavity and turbinates with extension of inflammation dorsally through the overlying bone into the subcutis and dermis. This latter possibility is considered less likely given the monomorphic population of debris-laden macrophages and the lack of sporangia or endospores within the dermis, subcutis and nasal bone that suggest previous resolution of infection at these sites rather than active spread. Further, chronic tissue remodeling would be expected within the nasal turbinates given the protracted disease progression of this case if the turbinates were the initial site of infection.

2. Fungal culture and phenotypic identification

Nasal turbinate tissue was cultured on Sabouraud dextrose agar (BD BBL, Franklin Lakes, NJ, USA), and on 5% sheep blood agar (Remel, San Diego, CA, USA) for 3 days of incubation at 25°C and 30°C. Lactophenol cotton blue and Gram stains were performed on isolated colonies. Matrix-assisted laser desorption ionization time of flight (MALDI-TOF) mass spectrometry analysis (VITEK MS – bioMérieux, Marcy-l'Étoile, France), and GEN III Microbial ID (Biolog, Hayward, CA, USA) analysis were performed as an attempt of genus/species identification. No ID was obtained, but the isolate assimilated: D-glucose, D-trehalose, acetic acid, weakly D-galactose, L-arabinose, glycerol, fructose and mannose.

3. Antimicrobials and antifungal susceptibility testing

Antimicrobial susceptibility testing was performed to determine the MIC (MIC) of 24 antimicrobials using Trek Sensititer COMPGP1 Gram positive panel (Trek Diagnostic Systems,

Cleveland, OH), according to manufacturer`s instructions. A suspension at 0.5 McFarland (10 ml) was used to inoculate the plate. Results were read visually after 24h of incubation at 30°C. Antifungal susceptibility testing was performed to determine the MIC of amphotericin B, fluconazole and itraconazol using Liofilchem MIC test strips with increasing concentration gradients of the antifungals (Liofilchem, Waltham, MA, USA), according to Clinical Laboratory Standards Institute (CLSI) document M27Ed4. Results were read visually after 24 and 48h of incubation at 30°C. All susceptibility tests were performed in duplicate. No universally accepted MIC interpretations of antimicrobials and antifungals specific for *Prototheca* species are available.

4. Sanger sequencing

Conventional pan-fungal PCR was performed targeting the internal transcribed spacer (ITS) region as well as the D1/D2 region of the large subunit of the 28S ribosomal RNA gene. *Aspergillus niger* ATCC 16404 was used as a positive control. PCR products were purified using the QIAquick PCR purification kit (Qiagen, Hilden, Germany) and sequenced by Sanger method at the AVDL (SeqStudio Genetic Analyzer, Thermo Scientific, Waltham, USA). BLAST (http://www.ncbi.nlm.nih.gov/BLAST) and the CBS-KNAW fungal database (http://www.westerdijkinstitute.nl/collections/) were used to identify related fungal sequences. Due to the rarity of *P. cutis* reports in the literature, we repeated the DNA extraction, PCR assays and sequencing. The second analysis yielded the same results and confirmed the presence of *P. cutis*.

5. Whole genome sequencing

Whole genome sequencing was carried out using the MiSeq platform (Illumina, San Diego, California), at the Athens Veterinary Diagnostic Laboratory (University of Georgia). DNA was obtained from the isolate grown on Sabouraud dextrose agar using a commercial kit, according to manufacturer’s instructions (ZR fungal/bacterial DNA MiniPrep, Zymo Research, Irvine, CA, USA). DNA concentration (17 ng/ml) was determined using a Qubit 2.0 fluorometer with a double-stranded DNA assay kit (Thermo Scientific, Waltham, MA, USA). A paired-end library with approximate insert size of 151 bp was prepared using Nextera DNA Flex library preparation kit (Illumina), and MiSeq reagent Kit v3 (150 cycles) chemistry according to the manufacturer’s protocol. The libraries were quality checked using a capillary electrophoresis device (QIAxcel, Qiagen).

The following *in silico* analyses were performed using the GenomeTrakr Network, GalaxyTrakr 1909 (https://www.galaxytrakr.org). The paired reads were first quality checked using Trimmomatic to remove adapters (Galaxy Version 0.36.4) and FastQC to select reads with Phred scores >30 (Galaxy Version 0.72+galaxy1). Assembly was performed using SPAdes software (Galaxy Version 3.12.0+galaxy1). The quality of assemblies was assessed using QUAST (Galaxy Version 5.0.2+galaxy0). Automated nuclear genome annotation was performed using Augustus (http://bioinf.uni-greifswald.de/augustus/submission.php), using *Chlamydomonas reinhardtii* as a reference species. Illumina MiSeq generated 2,008,194 paired-end reads with a genome coverage of ≈15x. The N50 read length was 5,846 bp and GC content was 61.07%. Plastid genome sequences were identified using BLAST against the chloroplast genome sequence of *P. cutis* ATCC PRA-338 (accession number: AP018373.1). Genome assemblies were imported into Geneious Prime (version 2020.1, https://www.geneious.com/prime/) for *in-silico* targeted gene evaluation. *P. cutis* genes of interest had their DNA sequences extracted from the whole genome assemblies. For that, sequences of *P. cutis* available in GenBank were aligned with whole genome assemblies from this study using Progressive Mauve aligner. These sequences included: ATCC PRA-338 partial *cytB* (599 bp, accession number MF163453.1), partial 28S rRNA (D1/D2 domain, 582 bp, accession AB470469.1), complete 18S rRNA gene (1,816 bp, accession MF163514.1), complete ITS (785 bp, accession KP898389.1), and complete plastid DNA genome (51,673 bp, accession AP018373.1).

Antimicrobial resistance genes were identified using the Comprehensive Antibiotic Resistance Database (CARD) with criteria selected as: perfect and strict hits only, excluding nudge of loose hits to strict, and high quality/coverage sequences (>70%) (https://card.mcmaster.ca/ accession 4/04/2020). The resistance genes were compared with phenotypic resistance to antimicrobials. As an attempt to identify antifungal resistance genes, we used the whole genome assemblies as input in the Mycology Antifungal Resistance Database (MARDY) (http://mardy.dide.ic.ac.uk/ accession 4/21/2020); however, no resistance genes were identified likely because of the lack of *Prototheca* in this database.

Reference

1. Masuda M, Jagielski T, Danesi P, Falcaro C, Bertola M, Krockenberger M, et al. Protothecosis in dogs and cats—new research directions. Mycopathologia. 2020 Nov 18 [Epub ahead of print]. PubMed

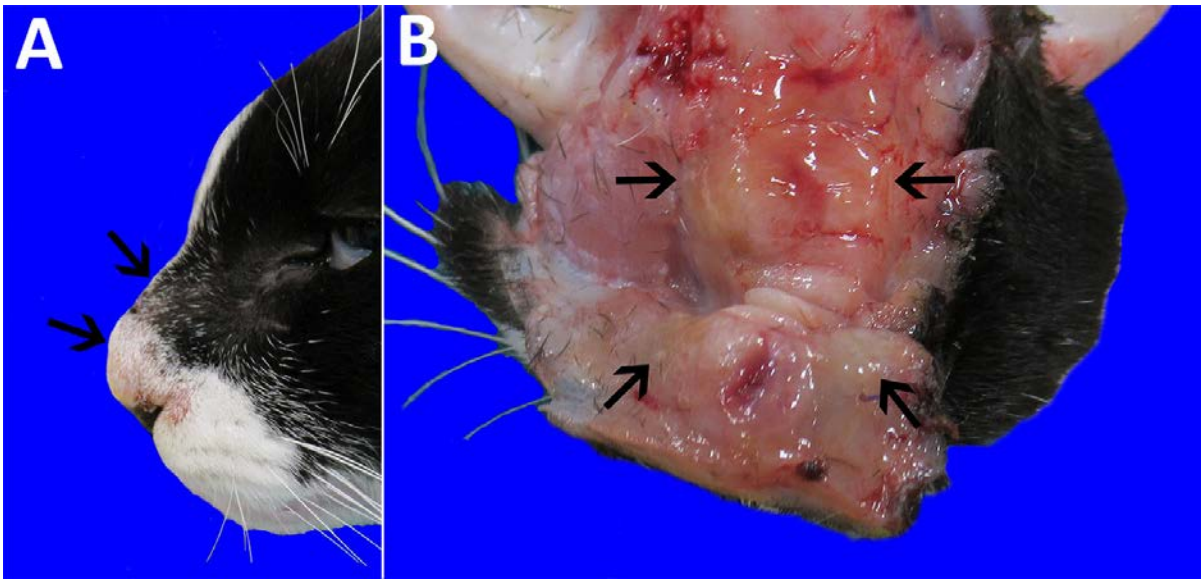

Appendix Figure 1. Gross lesions associated with protothecosis due to *Prototheca cutis* in a cat. A) Lateral view showing swelling and rounding of the nasal bridge. B) Dorsal view showing soft, tan to light orange, and mildly gelatinous connective tissue and musculature overlying the nasal bridge and dorsal nasal planum.

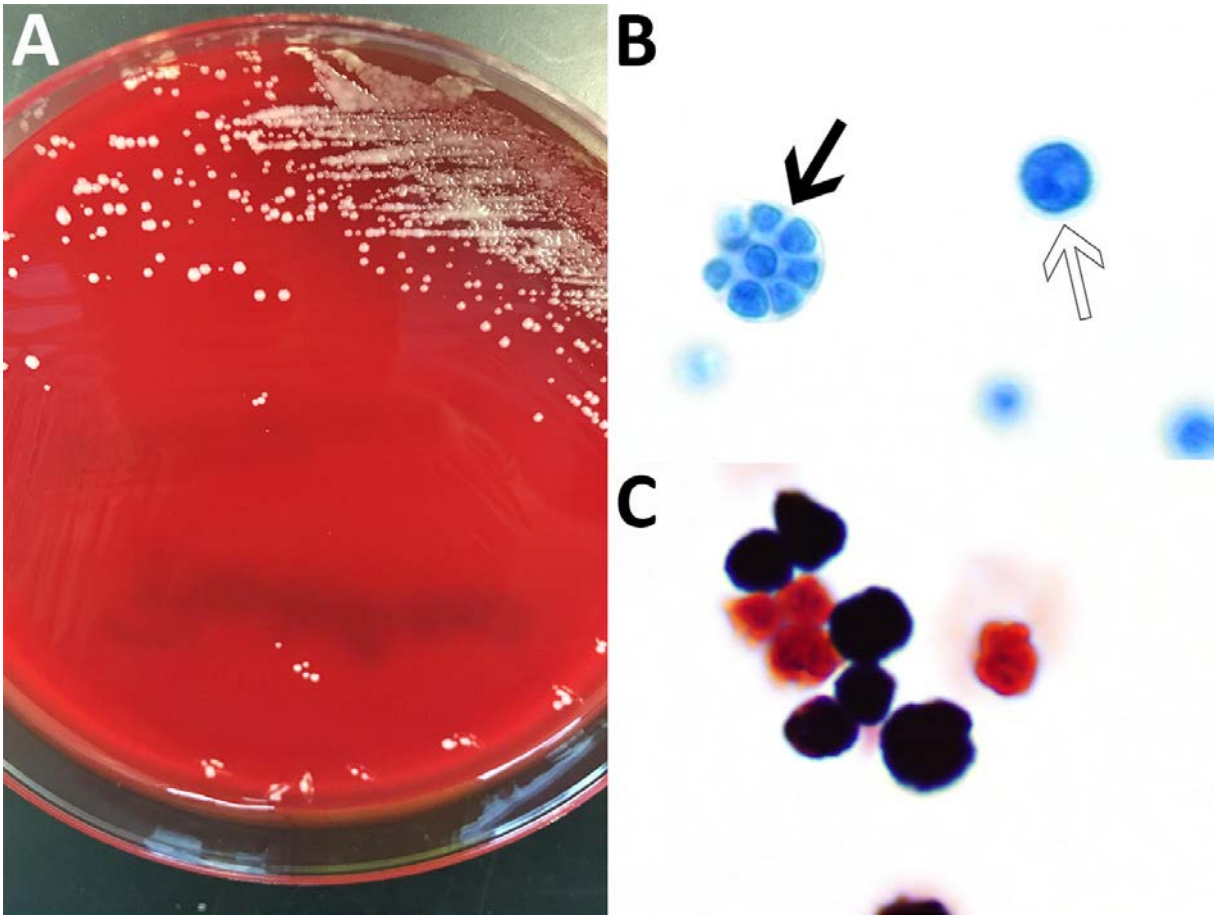

Appendix Figure 2. Culture results associated with protothecosis due to *Prototheca cutis* in a cat. A) Smooth and white colonies of *P. cutis* on sheep blood agar after incubation at 30°C for 72 h. B) Lactophenol cotton blue stain of *P. cutis* colonies showing the characteristic internal septations and thick cell walls of the sporangia, containing endospores (black arrow). During asexual reproduction, sporangiospores are released through a split which develops in the sporangial wall (arrowhead). Bar = 10 µm. C) Microscopic features of *P. cutis* revealing ovoid gram-positive cells, which are usually unevenly stained and do not show the characteristic internal septations. Bar = 10 µm.